

PREDICTING GAS-LIQUID FLOW IN A MECHANICALLY-STIRRED TANK

G. L. LANE, M.P. SCHWARZ

CSIRO Minerals, Box 312 Clayton Sth, Victoria 3169, Australia

G.M. EVANS

Dept of Chemical Engineering, University of Newcastle, New South Wales 2308, Australia

ABSTRACT

Computational fluid dynamics (CFD) provides a method for investigating the highly complex fluid flow in mechanically-stirred tanks. Although there are quite a number of papers in the literature describing CFD methods for simulating stirred tanks, most only consider single-phase flow. However, multiphase mixtures occur very frequently in the process industries, and these are more complex situations for which modelling is not as well developed. This paper reports on progress in developing CFD simulations of gas-liquid mixing in a baffled stirred tank. The model is three-dimensional and the impeller region is explicitly included using a Multiple Frames of Reference method to account for the relative movement between impeller and baffles. Fluid flow is calculated with a turbulent two-fluid model using a finite-volume method. Several alternative treatments of the multiphase equations are possible, including various expressions for drag and dispersion forces, and a number of these are being tested. Variation in bubble size due to coalescence and break-up is also modelled. The CFD simulation method has been used to model a gas-sparged tank equipped with a Rushton turbine, and simulation results are compared with experimental data. Results to date show the correct pattern of gas distribution and the correct trends in local bubble size in the tank.

Keywords: CFD, mixing, stirred vessel, two-phase flow, gas dispersion, bubble break-up, coalescence.

NOMENCLATURE

B_i	body force (N m^{-3})
C_{br}	adjustable coefficient in break-up rate (-)
C_{co}	adjustable coefficient in coalescence rate (-)
C_D	drag coefficient (-)
C_T	coefficient in dispersion equation (-)
D	bubble diameter (m)
d_p	particle diameter (m)
D_k	turbulent diffusivity ($\text{m}^2 \text{s}^{-1}$)
D_n	diffusivity coefficient in bubble eqn ($\text{m}^2 \text{s}^{-1}$)
D_{12}	diffusivity coefficient in drift velocity equation ($\text{m}^2 \text{s}^{-1}$)
F_i	interphase force (N m^{-3})
g	acceleration due to gravity (m s^{-2})
k	turbulent kinetic energy ($\text{m}^2 \text{s}^{-2}$)
n	bubble number per dispersion volume (m^{-3})
P	pressure (N m^{-2})
Re	Reynolds number (-)
S	source or sink of mass ($\text{kg m}^{-3} \text{s}^{-1}$)
T	time (s)
T_i	turbulent dispersion force (N m^{-3})

u_t	r.m.s. turbulent velocity (m s^{-1})
U_i	velocity (m s^{-1})
U_{slip}	slip velocity (m s^{-1})
V_d	drift velocity (m s^{-1})
We	Weber number (-)
X	position vector (m)
α_i	volume fraction (-)
ε	specific energy dissipation rate ($\text{m}^2 \text{s}^{-3}$)
η	efficiency factor (-)
λ	Kolmogorov microscale (m)
μ	viscosity (N s m^{-2})
ρ	density (kg m^{-3})
ρ_0	reference density (kg m^{-3})
σ	surface tension (N m^{-1})
Ω	angular velocity (rad s^{-1})

Subscripts

br	break-up
co	coalescence
crit	critical
i	phase number
L	laminar
T	turbulent
1	liquid
2	gas

INTRODUCTION

Computational fluid dynamics (CFD) is becoming an increasingly useful tool in the analysis of highly complex fluid flow in mechanically-stirred tanks. There are a number of papers published to date which present simulation methods for stirred tanks (e.g. Bakker, 1992; Tabor et al., 1996; Lane & Koh, 1997). However, most simulations reported in the literature deal with just single-phase liquid flow, whereas applications in the process industries often involve gas-liquid, solid-liquid, or three-phase mixtures, and hence modelling methods need to be extended to deal with multiphase flows. This paper describes progress in developing a simulation method for gas-liquid contacting in stirred tanks. It is intended that the model should be able to predict characteristics such as gas holdup, interfacial area, mass transfer rate and reaction rates. Such a model would have application in design and optimisation of a wide range of gas-liquid processes carried out in stirred vessels.

A number of simulations of gas-liquid dispersion in stirred tanks have been presented in the literature thus far, and although some degree of success is reported, a number of significant limitations are apparent. For

example, in several cases the model is axisymmetric, which is perhaps not very realistic (Morud & Hjertager, 1996; Jenne & Reuss, 1997; Zhu & Stokes, 1998), although three-dimensional simulations have also been carried out, notably by Bakker (1992). In several cases accuracy is probably limited by low grid resolution (e.g. Gosman et al., 1992). A constant bubble size is often assumed, although Bakker's method allows for bubble coalescence (Bakker, 1992). Another limitation common to all published methods is that the impeller is not directly simulated, but is instead modelled, for example using experimentally-determined impeller boundary conditions, in which case valid measurements must always be available. Also, such methods do not provide information about the flow in the impeller region.

Work is being undertaken to develop improved modelling methods for gas-liquid flow in stirred tanks. To make the method as independent as possible of experimental data, the impeller is explicitly included in the simulation. Emphasis is also given to obtaining the most efficient means of computation of such a complex flow, to determining the most appropriate models for the gas-liquid interaction, and predicting gas bubble sizes and interfacial area.

MODELLING THE IMPELLER

Literature on CFD modelling of baffled stirred tanks demonstrates a range of modelling methods, one of the main variations being in the treatment of the impeller-baffle interaction, where a significant modelling problem arises since there is no single frame of reference for carrying out computations. In some cases an empirical model is provided for the impeller, as in gas-liquid simulations reported thus far (e.g. Bakker 1992; Jenne & Reuss, 1997). However, several methods are reported for single-phase flow which treat the impeller region explicitly and these might possibly be extended to two-phase flow. The Sliding Mesh method has been widely used in recent years (e.g. Lane & Koh, 1997). This is a time-dependent method where the section of the grid surrounding the impeller is allowed to rotate stepwise, and the flow field is recalculated for each step. This method is therefore very computationally intensive, and computational requirements become excessive for two-phase flow. An alternative method is the Multiple Frames of Reference method, where flow is calculated by dividing the tank into two domains each with its own frame of reference. In the impeller region flow is calculated in a rotating frame of reference where the impeller appears stationary, while in the bulk of the tank a stationary frame of reference is used, a correction in the velocities being made at the interface between the two zones. Thus, a steady-state calculation can be carried out. For single-phase flow, the method has previously been shown to provide a saving in computer time of a factor of about 10, while providing a degree of accuracy similar to the Sliding Mesh method (Luo et al., 1994; Tabor et al., 1996). Therefore, to permit more efficient computation, this method has been adopted here and extended to two-phase flow.

EQUATIONS FOR TWO-PHASE FLOW

Gas-liquid flow is modelled using a two-fluid approach where the gas and liquid are described as interpenetrating

continua and equations for conservation of mass and momentum are solved for each phase. However, since the flow is turbulent, the equations are solved in an averaged form requiring a turbulence model for closure. The equations for each phase, i ($= 1$ for liquid, $= 2$ for gas), are as follows:

$$\frac{\partial(\alpha_i \rho_i)}{\partial t} + \nabla \cdot (\alpha_i \rho_i \bar{U}_i - \rho_i D_i \nabla \alpha_i) = S_i \quad (1)$$

$$\begin{aligned} & \frac{\partial(\alpha_i \rho_i \bar{U}_i)}{\partial t} + \nabla \cdot ((\alpha_i \rho_i \bar{U}_i \otimes \bar{U}_i) \\ & - \alpha_i (\mu_{L,i} + \mu_{T,i}) (\nabla \bar{U}_i + (\nabla \bar{U}_i)^T)) \\ & = -\alpha_i \nabla P_i + \alpha_i (\rho_i - \rho_0) \bar{g} + \bar{F}_i + \bar{B}_i + \bar{T}_i + S_i \bar{U}_i \end{aligned} \quad (2)$$

The turbulent viscosity $\mu_{T,i}$ in the liquid phase is calculated using the standard $k-\epsilon$ turbulence model, whereas $\mu_{T,i}$ is assumed zero for the gas. The term \bar{B}_i represents the centrifugal and Coriolis forces which apply in the rotating frame of reference only and are given by:

$$\bar{B}_i = -2\alpha_i \rho_i \bar{\Omega} \otimes \bar{U}_i - \alpha_i \rho_i \bar{\Omega} \otimes (\bar{\Omega} \otimes \bar{X}). \quad (3)$$

The term S_i (for $i=2$) is the mass source or sink of gas at the sparger and liquid surface, \bar{F}_i is the generalised interphase force and \bar{T}_i is the turbulent dispersion force.

There is a lack of agreement in the literature as to the exact form of the equations, with differences due to the assumed form of the instantaneous equations, due to the averaging method applied, and also due to differences in closure terms for the turbulent correlations which arise after averaging. These differences relate mostly to modelling of turbulent dispersion and interphase forces, and thus may have a large influence on predictions of gas distribution and holdup.

For modelling of turbulent dispersion, one approach taken uses the Reynolds-averaged equations, where turbulent dispersion is specified by the diffusive term in equation (1) and D_k , the turbulent diffusivity, is usually set as a constant ratio to the liquid turbulent viscosity. However, Bakker (1992) provides an alternative equation for this diffusive term. Alternatively, if the equations are Favre-averaged, D_k in equation (1) is set to zero and turbulent dispersion appears as a force in the momentum equation. One possible expression is (Viollet and Simonin, 1994):

$$\bar{T}_2 = -\bar{T}_1 = C_T \rho_1 k \nabla \alpha_2. \quad (4)$$

In modelling the interphase forces, \bar{F}_i , the drag force is the most important, although forces such as added mass and lift may also need to be included. The drag force may be written as:

$$\bar{F}_d = \frac{3}{4} \frac{C_D}{d} \alpha_1 \alpha_2 \rho_1 |\bar{U}_{slip}| \bar{U}_{slip}. \quad (5)$$

For calculation of the drag coefficient C_D , the correlation of Ishii and Zuber (1979) is frequently used for bubbles. This correlation has been applied in modelling gas flow in stirred tanks (e.g. Gosman et al., 1992; Morud &

Hjertager, 1996; Jenner & Reuss, 1997), however correlations such as this have been developed for bubbles or particles in stagnant liquids and may not be adequate where there is a high level of forced turbulence, as in a stirred tank. There is a strong interaction between bubbles and turbulent eddies, where the bubbles are continually being accelerated by eddies of different sizes and velocities. This may modify the relative mean velocity between gas and liquid, so that the effective drag force cannot be calculated by standard correlations. Available data indicate that the effect of turbulence may be quite large (Brucato et al., 1998). Based on measurements for solid particles up to 500 μm , it was found (Brucato et al., 1998) that the drag coefficient, C_D , under turbulent conditions could be correlated by:

$$\frac{C_D - C_{D,0}}{C_{D,0}} = 8.76 \times 10^{-4} \left(\frac{d_p}{\lambda} \right)^3 \quad (6)$$

where $C_{D,0}$ is the drag coefficient in a stagnant fluid and λ is the Kolmogorov microscale of turbulence.

In another approach (Bakker, 1992), a standard correlation is used for drag coefficient but the effect of turbulence is accounted for by calculating a modified Reynolds number as a function of turbulent eddy viscosity, defined as:

$$\text{Re}^* = \frac{\rho_1 \bar{U}_{slip} d}{\mu_L + \frac{2}{9} \mu_{T,1}} \quad (7)$$

In yet another approach, the drag coefficient has been calculated by “standard” correlations, but the slip velocity is calculated differently (Gosman et al., 1992; Viollet & Simonin, 1994). By taking into account the biasing in averaging due to inhomogeneous gas distribution, the average slip may be written as:

$$\bar{U}_{slip} = [\bar{U}_2 - \bar{U}_1] - \bar{V}_d \quad (8)$$

where \bar{V}_d is the drift velocity, which may be modelled in terms of the gradient of volume fraction according to:

$$\bar{V}_d = - \frac{D_{12}}{\alpha_1 \alpha_2} \nabla \alpha_2 \quad (9)$$

Work is in progress to test these various alternative approaches to the equations for gas-liquid flow.

BUBBLE BREAK-UP AND COALESCENCE

Another complexity is the prediction of bubble size, which is required for calculation of interfacial area and interphase transfer of momentum, mass and energy. The approach taken here is to calculate bubble number density, n , which is a measure of local average bubble size. An additional transport equation is solved for n , accounting for transport of bubbles (by convection and turbulent diffusion) and changes in bubble size (and therefore bubble number) by break-up and coalescence according to:

$$\frac{\partial n}{\partial t} + \nabla \cdot (n \bar{U}_2 - D_n \nabla n) = S_{br} - S_{co} \quad (10)$$

where S_{br} and S_{co} are the source and sink terms describing break-up and coalescence rates respectively.

In modelling coalescence (Prince & Blanch, 1990; Bakker, 1992; Wu et al., 1998), it is generally considered that coalescence occurs due to binary collisions between bubbles, and expressions for collision rate are derived by assuming random collisions induced by turbulent eddies, analogous to the model for molecular collisions in the kinetic theory of an ideal gas. Hence the coalescence rate term has the following form:

$$S_{co} \propto d^2 u_t n^2 \quad (11)$$

Here, u_t is taken to be the velocity of eddies in the inertial subrange of the turbulent eddy spectrum, which may be written as:

$$u_t = 1.4 (\epsilon d)^{1/3} \quad (12)$$

An additional factor should be introduced to account for the reduced mean free path of bubbles with increasing gas volume fraction, α_2 (Wu et al., 1998), so that the expression for coalescence rate becomes:

$$S_{co} = C_{co} \eta_{co} d^2 (\epsilon d)^{1/3} n^2 \cdot \frac{1}{(1 - \alpha_2^{1/3})} \quad (13)$$

where η_{co} is the coalescence efficiency, which is set to unity for the time being.

The tendency for bubbles to break up or remain stable may be defined in terms of a Weber number, being the ratio of the disruptive forces to the restoring surface tension force, given by:

$$\text{We} = \frac{\rho u_t^2 d}{\sigma} \quad (14)$$

Bubble break-up occurs only when the Weber number exceeds a critical value, We_{crit} , which is approximately 1.2 in turbulent flows (Rigby et al., 1997). However, an expression is also needed for the rate of bubble break-up, which may be considered to depend on the frequency of collisions between bubbles and eddies of a similar size (Prince & Blanch, 1990; Wu et al., 1998). Furthermore, the fraction of eddies with sufficient energy may be estimated as an exponential function. These considerations lead to the following expression for the break-up rate (Wu et al., 1998), which is used in the current modelling approach:

$$S_{br} = C_{br} n \frac{(\epsilon d)^{1/3}}{d} \left(1 - \frac{\text{We}_{crit}}{\text{We}} \right)^{1/2} \exp \left(- \frac{\text{We}_{crit}}{\text{We}} \right), \quad (15)$$

$\text{We} > \text{We}_{crit}$

SIMULATION METHOD

The CFD model was set up to simulate a gas-sparged tank for which published experimental data is available for the distribution of bubble sizes and local gas holdup (Barigou and Greaves, 1992 & 1996). Specifically, the gas is air and the liquid is water, and properties are set in the model accordingly. The tank is baffled and has a 1.0 m diameter with a standard Rushton turbine 0.333 m diameter located at a clearance of 0.25 m. Impeller speed

is set to 180 rpm and the gas flow rate is 0.00164 m³/s. The tank is modelled by a finite volume grid in cylindrical coordinates (see Figure 1), with 61, 36 and 20 cells in the axial, radial and azimuthal directions respectively. To reduce the problem size, one sixth of the tank is modelled, including just one blade and one baffle with periodic boundary conditions assumed in the azimuthal direction. All walls are treated as no-slip boundaries applying wall functions to calculate the velocity profiles near the wall, except that the liquid surface is treated as a zero stress boundary. Gas is added at the sparger and removed at the liquid surface using source terms in the equations. The bubbles at the inlet are assumed to have a mean size of 2 mm.

The set of equations are solved numerically using the commercial code CFX4.2. The code has been augmented by several user-supplied routines, to implement the Multiple Frames of Reference method; to add and remove gas from the tank; and to specify equations for turbulent dispersion, interphase forces, and bubble number density. Satisfactory completion of each simulation is based on sufficient reduction of the mass residuals, and also the rates of gas entering and leaving must be equal and the calculated holdup must attain a constant value.

RESULTS AND DISCUSSION

Simulations of the gas-sparged tank have been run using several possible versions of the two-phase equations with different terms for turbulent dispersion and drag force, in each case comparing the results with the published experimental data (Barigou and Greaves, 1992). For the best results to date as presented here (see Figures 2 – 5), the turbulence dispersion is specified in terms of the turbulent dispersion force, equation (4), (with D_k set to zero in equation (1)), and the drag force is calculated using the modified slip velocity in terms of the drift velocity (equation 8). For the calculation of drag coefficient the correlation of Ishii and Zuber, 1979 was used, however this was based on the unmodified slip velocity, since including drift velocity in calculating drag coefficient led to erroneous results.

Figure 2 shows the liquid phase velocity field under two-phase conditions, indicating the well-known pattern of flow with radial discharge from the impeller. Figure 3 indicates the gas volume fraction in a vertical slice. The pattern of gas distribution corresponds quite well with the experimental measurements. The gas rises into the impeller and is then dispersed into the bulk of the tank. Most of the gas holdup is in the section of the tank above the impeller and is fairly evenly dispersed. In the lower part of the tank and close to the impeller there is a region free of gas. Figure 4 shows the pressure distribution in a horizontal plane through the impeller, where there is a large pressure difference between lead and trailing sides of the impeller blade. As shown in Figure 5, gas accumulates in this low pressure region behind the impeller blade, before being dispersed by the highly turbulent impeller discharge stream.

Although the pattern of gas distribution appears correct, the total gas holdup is underpredicted at present. It is probable that this is due to the use of the correlation for

drag coefficient according to Ishii and Zuber (1979), which may not be appropriate since the drag coefficient may be affected by the turbulence. Further simulations have been carried out to test other equations for the drag coefficient as proposed in the literature, namely the equations of Brucato et al. (1998) (equation 6) and Bakker (1992) (equation 7). Both methods predict higher gas holdup, however the results were unsatisfactory since the predicted pattern of gas distribution was wrong in both cases, giving too much gas near the bottom of the tank.

Figure 6 shows the predicted distribution of bubble sizes in a vertical slice through the tank. It is seen that bubbles are largest in the high gas fraction plume leading from the sparger to the impeller. In the impeller discharge, smaller bubbles are generated due to break-up in the highly turbulent impeller discharge stream, while above and below the impeller stream the bubbles become larger again due to coalescence. The pattern is quite similar to that found experimentally, however predicted bubble sizes in the bulk of the tank are generally smaller than the typical experimental values of between 3 – 4 mm. To obtain more accurate results, it is necessary to improve the prediction of the variables used as input in the bubble number density equation, and as well it is likely that some further development of the rate expressions for coalescence and break-up is needed.

CONCLUSIONS

A CFD simulation method is being developed to model gas-liquid dispersion in mechanically-agitated mixing vessels. The impeller is included in the simulation and therefore experimental data for the impeller is not needed. The Multiple Frames of Reference method is implemented, allowing for efficient calculation in steady-state mode. Several models for interphase drag and turbulent dispersion have been tested and bubble size is also predicted. Results to date indicate the correct patterns of liquid velocity, gas distribution and bubble size throughout the vessel. Development of the modelling is continuing, so as to provide better quantitative agreement with experimental measurements of gas holdup and bubble size, by further development of the models for gas-liquid interphase forces and turbulent dispersion, and improved prediction of bubble breakup and coalescence rates

REFERENCES

- BAKKER, A., 1992, *Hydrodynamics of Stirred Gas-Liquid Dispersions*, Ph.D. Thesis, Delft University of Technology, The Netherlands.
- BARIGOU, M. and GREAVES, M., 1992, "Bubble-size distributions in a mechanically agitated gas-liquid contactor", *Chem. Eng. Sci.*, Vol. 47, No. 8, pp. 2009–2025.
- BARIGOU, M. and GREAVES, M., 1996, "Gas holdup and interfacial area distributions in a mechanically agitated gas-liquid contactor", *Trans. I. Chem. E.*, Vol. 74, Part A, pp. 397–405.
- BRUCATO, A., GRISAFI, F. and MONTANTE, G., 1998, "Particle drag coefficients in turbulent fluids", *Chem. Eng. Sci.*, Vol. 53, No. 18, pp. 3295–3314.

GOSMAN, A.D., LEKAKOU, C., POLITIS, S., ISSA, R.I., and LOONEY, M.K., 1992, "Multidimensional Modeling of Turbulent Two-Phase Flows in Stirred Vessels", *AIChE Journal*, Vol. 38, No. 12, pp. 1946–1956.

ISHII, M. and ZUBER, N., 1979, "Drag Coefficient and Relative Velocity in Bubbly, Droplet or Particulate Flows", *AIChE Journal*, Vol. 25, No. 5, pp. 843–855.

JENNE, M. and REUSS, M., 1997, "Fluid Dynamic Modelling and Simulation of Gas-Liquid Flow in Baffled Stirred Tank Reactors", *Recent Progresses in Genie des Procedes*, Vol. 11, No. 52, pp. 201–208.

LANE, G. and KOH, P.T.L., 1997, "CFD Simulation of a Rushton Turbine in a Baffled Tank", *Proc. Int. Conf. on Comp. Fluid Dynamics in Mineral & Metal Processing & Power Generation*, CSIRO, Melbourne, 3-4 July 1997, pp. 377–385.

LUO, J.Y., ISSA, R.I., and GOSMAN, A.D., 1994, "Prediction of Impeller Induced Flows in Mixing Vessels Using Multiple Frames of Reference", *I Chem E Symposium Series*, No. 136, pp. 549–556.

MORUD, K.E., and HJERTAGER, B.H., 1996, "LDA Measurements and CFD Modelling of Gas-Liquid Flow in a Stirred Vessel", *Chem. Eng. Sci.*, Vol. 51, No. 2, pp. 233–249.

PRINCE, M.J., and BLANCH, H.W., 1990, "Bubble Coalescence and Break-Up in Air-Sparged Bubble

Columns", *AIChE Journal*, Vol. 36, No. 10, pp. 1485–1499.

RigBy, G.D., EVANS, G.M., and JAMESON, G.J., 1997, "Bubble breakup from ventilated cavities in multiphase reactors", *Chem. Eng. Sci.*, Vol. 52, Nos. 21/22, pp. 3677–3684.

TABOR, G., GOSMAN, A.D., and ISSA, R.I., 1996, "Numerical Simulation of the Flow in a Mixing Vessel Stirred by a Rushton Turbine", *Fluid Mixing V, I.Chem.E. Symposium Series*, No.140, pp. 25–34.

VIOLLET, P.L. and SIMONIN, O., 1994, "Modelling dispersed two-phase flows: Closure, validation and software development", *Applied Mechanics Review*, Vol. 47, No. 6, pp. S80–S84.

WU, Q., KIM, S., IsHii, M., and BEUS, S.G., 1998, "One-group interfacial area transport in vertical bubbly flow", *Int. J. Heat Mass Transfer*, Vol. 41, Nos. 8-9, pp. 1103–1112.

ZHU, Z. and STOKES, N., 1998, "Predicting Turbulent Gas-Liquid and Solid-Liquid Multi-Phase Flows in a Stirred Mixing Tank", Chemeca '98, Port Douglas, Australia.

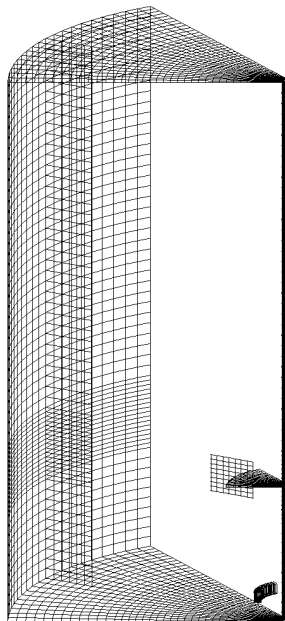


Figure 1: Finite volume grid for 60° tank section.

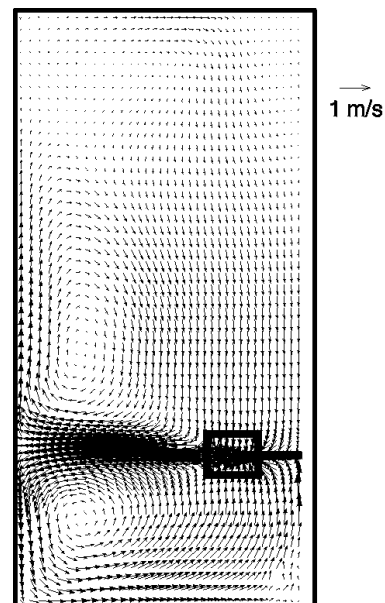


Figure 2: Velocity vectors for liquid in two-phase flow – vertical plane through centre of tank 28° behind impeller blade.

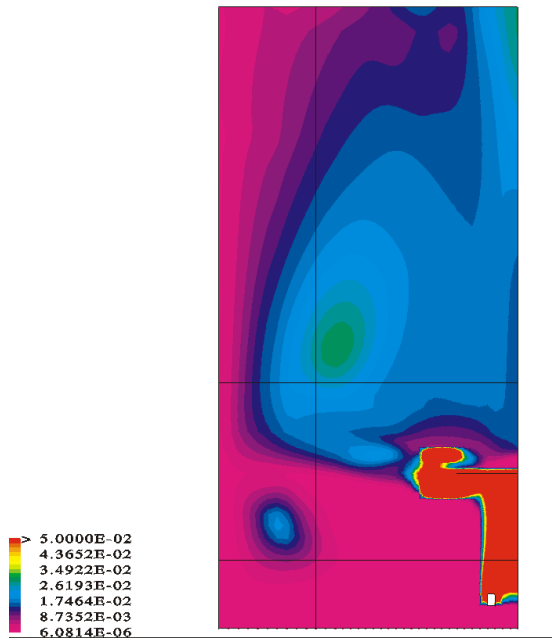


Figure 3: Gas volume fraction in vertical plane 2° behind impeller blade.

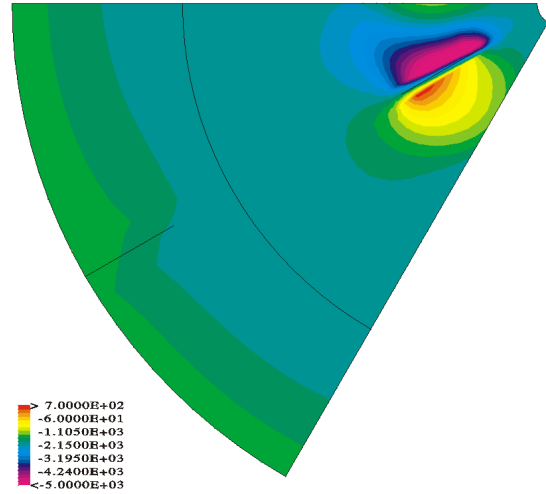


Figure 4: Pressure distribution (Pa) in a horizontal plane through the impeller (at $\frac{3}{4}$ of blade height).

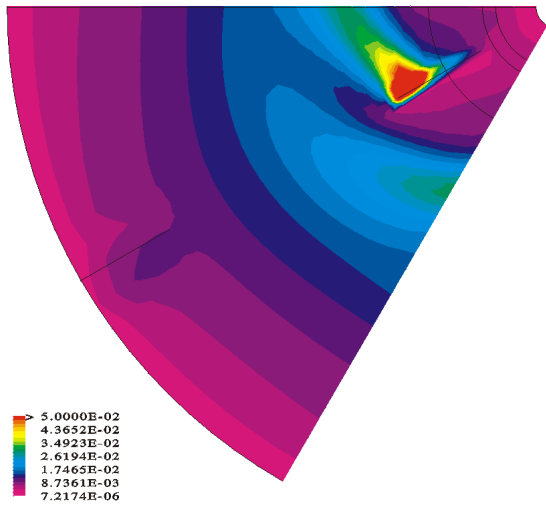


Figure 5: Gas volume fraction in a horizontal plane through the impeller (at $\frac{3}{4}$ of blade height).

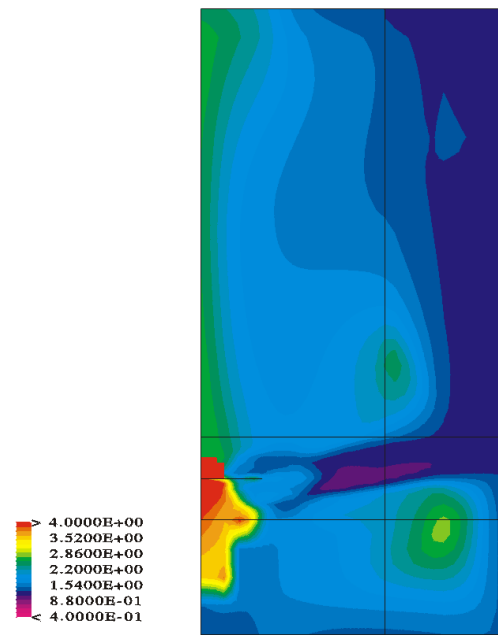


Figure 6: Bubble diameter (mm) in plane half way between impeller blades